

IRAC1_PR4x_300.fits

David Makovoz, 09/27/05

New PRF for IRAC1

Estimating PRF for IRAC1 is a challenging task, since the data is undersampled. The basic steps of PRF estimation are described in `prf_estimate.doc`. They are: finding point sources suitable for PRF estimation, cutting out individual point source images from the bcd's, centering the individual point source images, shifting them, performing outlier rejection, creating individual prf images by shifting and resampling individual point source images while taking into account the outlier information, and finally combining the individual prf's into one PRF image.

For undersampled data centering and interpolation are more complicated. Three new procedures have been implemented to deal with undersampled data. They are:

1. Sparse interpolation described in Appendix 1.
2. Using the mosaic extraction table to determine the point source coordinates as described in Appendix 2.
3. Residual image refinement described in Appendix 3.

A new PRF was derived from the bcd's of 8 xfls AOR's :

(3861504, 3861760, 3862272, 3862528, 3862784, 3863040, 3863296 , 3863552).

There were a total of ~4500 point source images with fluxes ranging from 1mJy to 10 mJy for 95% of those sources. The lower limit on the point source fluxes was enforced explicitly, the high flux sources were rejected based on the χ^2/dof threshold.

The basic algorithm produced a PRF which is referred to as PRF_0. The three improvements described above produced three PRF's: PRF_1, PRF_2, and PRF_3. The sparse interpolation alone produced PRF_1. The sparse interpolation combined with using the mosaic extraction table for the point source coordinates produced PRF_2. Subsequently applying the residual image refinement to PRF_2 produced PRF_3. These PRF's were resampled with the factor 4, because there were not enough data for resampling factor of 8 for the sparse interpolation option

The PRF derived from the 100 bcd's of the dedicated AOR, known as `IRAC1_Short_PR4x_jan05.fits` was compared with the new PRF's. In order to obtain a quantitative comparison of the PRF's point source extraction was performed on the data from AOR 5712384. The sources with $\chi^2/dof < 1000$ were saved in the source lists.

Table 1 contains the number of sources in the list, the mean, median, and mode of the χ^2/dof for the extraction lists obtained with 5 versions of the PRF.

PRF version	N_sources	Mean	Median	Mode
PRF_jan05	28142	50.0	9.0	3.9
PRF_0	28074	49.6	9.2	3.9
PRF_1	28860	44.1	7.8	4.2
PRF_2	29108	30.5	6.5	3.3
PRF_3	29216	27.3	6.3	3.1

Table 1 Mean, median, and mode of the χ^2/dof distribution obtained by fitting AOR 5713484 with various PRF's.

A direct comparison of the point source extraction results for PRF_3 and IRAC1_Short_PRF8x_jan05.fits was performed. The two extraction lists were matched creating a list of sources extracted with both PRF's. The combined list contained 27697 sources. The histograms of the χ^2/dof are shown in Fig.1.

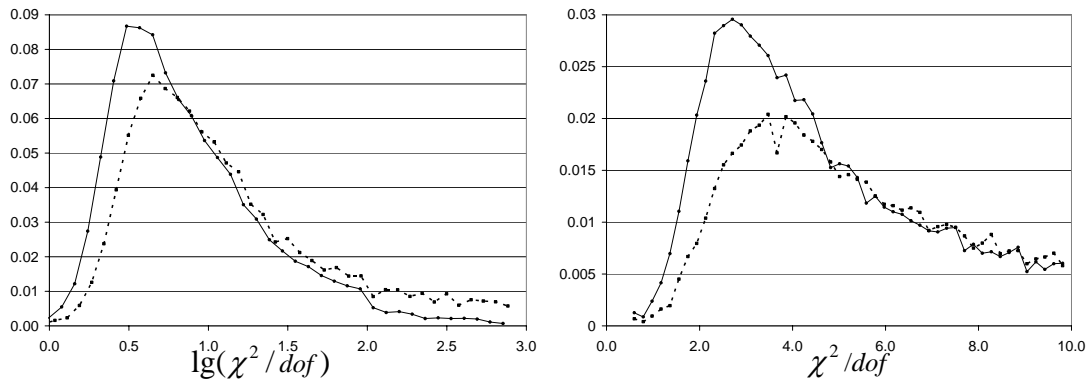


Figure 1. The histogram of the χ^2/dof values for the PRF_3 (solid line) and PRF_jan05 (dotted line).

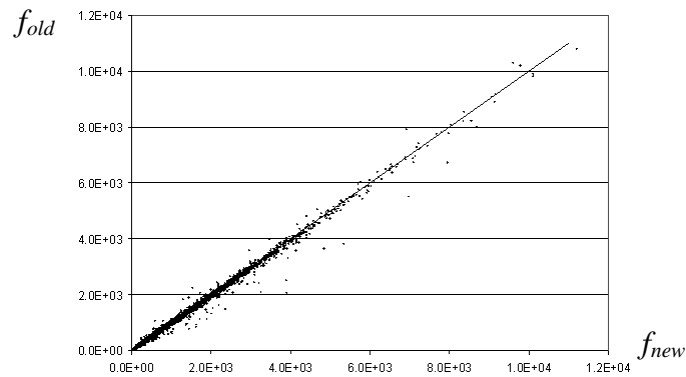


Figure 2. Flux f_{old} obtained with IRAC1_Short_PRF8x_jan05.fits vs. f_{new} obtained with PRF_3. The straight line has the slope of 1.

The good news is that the flux obtained with IRAC1_Short_PRF8x_jan05.fits doesn't have any systematic error compared with the flux obtained with PRF_3 (see Fig. 2).

PRF_3 is included in the current MOPEX distribution under the name of IRAC1_PRF4x_300.fits.

Appendix 1. Sparse Bicubic Interpolation

A PRF is a continuous function of the pixel position with respect to the point source. For practical purposes a PRF is saved as a discrete set of values of the pixel responses to a point source measured on a regular grid of points. The point source is normally assumed to be at the central grid point. In Fig. 3 we show an example of a grid of the points i with coordinates (x_i, y_i) at which the PRF is being estimated. The star shows the point source position (x_o, y_o) . A PRF is estimated by combining individual point source images s^a . Each image s^a represents the PRF measured at some arbitrary points determined by the point source position with respect to the grid. 16 pixels of such an image are shown in Fig. 3, where the big circles are the centers p of the pixels of image s^a with coordinates (x_p, y_p) . The pixel values of image s^a represent the measurements of the PRF at the points marked with the big circles.

For each point source image a an individual prf^a image is created by performing the bicubic interpolation of the values of the point source image s^a . The value of prf^a at position j is a linear combination of the 16 values of s^a :

$$prf^a(i) = \sum_{p=1}^{16} C(i, p) s^a(p) \quad (A1)$$

at the 16 positions p closest to i . The coefficients $C(i, p)$ depend on the distance between the points i and p :

$$C(i, p) = h(x_i - x_p) h(y_i - y_p); \quad (A2)$$

Interpolation (A2) is equivalent to shifting the observed image s^a to the grid positions i . Here we deal with undersampled data. One should minimize the shift in order to reduce the errors introduced by such a shift. The sparse interpolation is designed to address this problem. For the sparse interpolation the PRF is evaluated only at the grid points i closest to the points p , at which the actual measurements are taken. In Fig. 3 these points are marked with boxes. Others points are left uninitialized. In order to keep track of which points are computed in each prf^a , a separate array of values cvg^a is kept. The value of $cvg^a(i)$ is set to 1, if $prf^a(i)$ is interpolated for image a , and it is set to 0 otherwise.

The individual prf^a images are combined in order to create the final PRF image:

$$\begin{aligned} PRF(i) &= \frac{1}{N(i)} \sum_a prf^a(i); \\ N(i) &= \sum_a cvg^a(i) \end{aligned} \quad (A3)$$

Here the number of points in the stack $N(i)$ can be different for different grid positions i , especially if the sparse interpolation is performed.

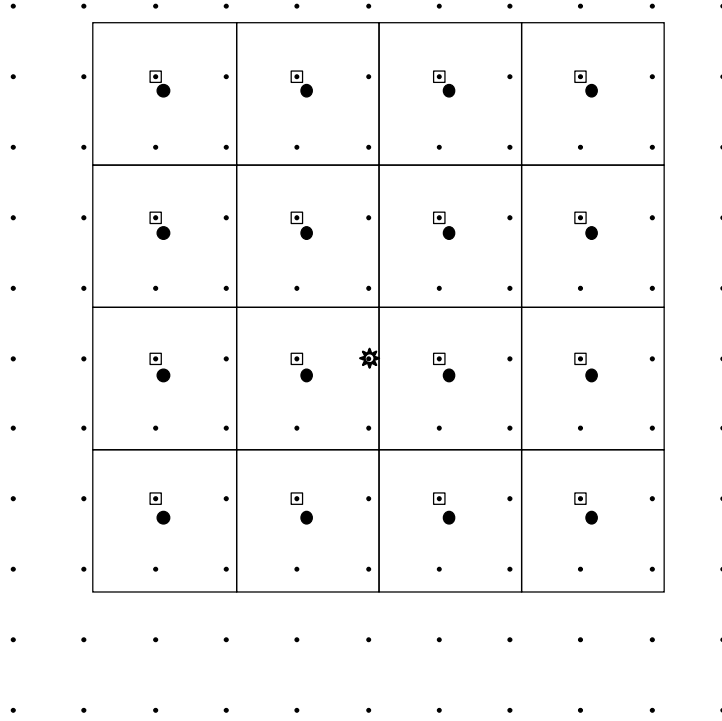


Figure 3. The *PRF* is evaluated at the grid positions shown with the dots. The star shows the location of the point source. The circles represent the centers of the pixels of the observed image, which are shown as the squares. The value at each dot is interpolated from the 16 closest big circles. For the sparse interpolation only the closest small points are evaluated; these points are marked with boxes.

Appendix 2. Point Source Positions from Mosaic Point Source Extraction

The individual point source images S^a are to be combined into one *PRF* image. Before they can be combined they should be shifted to a common grid. The images should also be normalized by their fluxes in order to perform outlier detection.

The simplest way of estimating the position of the point sources \mathbf{r}_c^a and their fluxes f^a in a point source image a is by finding the flux weighted centroids and the total flux in each image:

$$f^a = \sum_i S^a(i); \quad \mathbf{r}_c^a = \frac{\sum_i S^a(i)\mathbf{r}_i}{f^a}; \quad (\text{A4})$$

where the summation is performed over the pixels i in the central part of the point source image, $\mathbf{r}_i \equiv (x_c, y_c)$ are the coordinates of the center of pixel i . Another option is fitting the images with some model. Initially such a model can be a 2D Gaussian:

$$G(i) = \frac{f}{2\pi\sqrt{\text{Det}(\Theta)}} \exp\left(-\frac{1}{2}\left((x_i - x_c)^2 \Theta^{-1}_{xx} + (y_i - y_c)^2 \Theta^{-1}_{yy} + 2(x_i - x_c)(y_i - y_c) \Theta^{-1}_{xy}\right)\right)$$

$$\Theta = \begin{vmatrix} \sigma_x^2 & \sigma_{xy}^2 \\ \sigma_{xy}^2 & \sigma_y^2 \end{vmatrix}$$
(A5)

We fit the data by minimizing the good-of-fit measure χ^2 defined as

$$\chi^2 = \sum_{i \in W} (S^a(i) - G(i, \mathbf{r}_c^a, f^a, \Theta))^2 .$$
(A6)

W is the fitting area, a square normally set to be 5 by 5 pixels. The fitting parameters are the flux f^a , and position \mathbf{r}_c^a of the point source along with shape of the 2D Gaussian Θ .

The third option of estimating the fluxes and positions of the point sources in each point source image becomes available once the initial estimate of *PRF* is obtained. Then one can do *PRF* fitting of the data by minimizing χ^2 defined as:

$$\chi^2 = \sum_{i \in W} (S^a(i) - f^a \text{PRF}(i, \mathbf{r}_c^a))^2 ,$$
(A7)

where W is the fitting area defined the same way as in Equation (A6).

The individual point source images are normalized by the flux f^a obtained by fitting:

$$s^a(i) = S^a(i) / f^a ,$$
(A8)

where s^a are the normalized point source images.

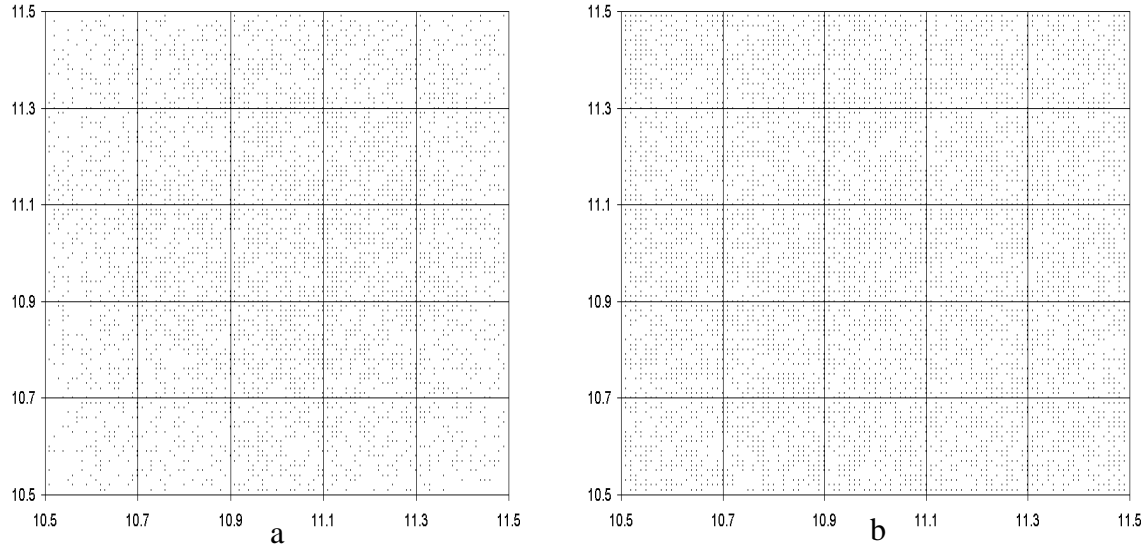


Figure 4. The point source positions within the central pixel obtained by centroiding (a) and by projecting the mosaic point source coordinates (b).

It turned out that all of the above methods produce biased results for the point source positions. The scatter plot of the point source positions obtained by centroiding is shown in Fig. 3a. The point source distribution within the pixel is not uniform.

The most reliable estimation of the point source positions is using the point source coordinates obtained by doing the point source extraction in the mosaic image and then projecting the sky coordinates onto the individual frames. Fig.3b shows that the point source distribution is mostly uniform in this case.

To obtain a quantitative comparison of different methods the offsets δX_c , δY_c of the average point source positions X_c and Y_c from the pixel center were computed for the four methods and are presented in Table 2. Table 2 also contains the *RMS* of the point source coordinates defined as:

$$RMS = \sqrt{\frac{2}{N} \sum_i (x_i - X_c)^2 - (y_i - Y_c)^2} \quad (A9)$$

Here the summation is done over N point sources with coordinates (x_i, y_i) . The ideal case of the uniformly distributed source has the *RMS* ~ 0.41 .

Method	δX_c	δY_c	<i>RMS</i>
2D Gaussian fitting	0.05	0.00	0.32
Centroids	0.02	0.02	0.36
Single frame PRF fitting	0.00	0.00	0.38
Mosaic coordinates	0.00	0.00	0.40

Table 2. The offsets - δX_c , δY_c -of the average point source positions, and the *RMS* of the point source positions are computed with 4 different methods.

Appendix 3. Residual Image Refinement

It was observed that the residual mosaic had a certain pattern: the central pixel was undersubtracted and the pixels around it were oversubtracted. This is an indication that the PRF is not sharp enough. The following procedure was applied to fix this problem and improve the residual images. From the list of extracted sources the non-confused sources with the flux > 1 mJy were selected. The residual bcd's were created by subtracting these point sources. The postage stamp images 21x21 pixels were cut out from the residual bcd's for all the selected point sources. The median of the stack of the postage stamp images was computed. Also the median of all the fluxes of the selected point sources was computed. The median image was normalized by the median flux. The normalized median was subtracted from the PRF_2. The procedure of point source extraction and subtracting the normalized median was repeated three times. The result of this procedure is PRF_3.



Figure 5. The median of the residual point source images for the PRF_2 (left) and PRF_3 (right). The images are shown on the same scale.